Measurements, Simulations, and Optimization of an ALMA Band 5 Vacuum Window Prototype

Arne Schröder*, Axel Murk*, Pavel Yagoubov† and Ferdinand Patt†
*Institute of Applied Physics, University of Bern, Bern, Switzerland
†European Southern Observatory, ALMA Front End Division, Garching, Germany

***Abstract*—This work analyzes the reflectivity and transmittance of a vacuum window prototype for the ALMA Band 5 by using numerical and experimental tests. Simulations are carried out with the finite element method and an efficient semi-analytical technique. Geometrical inaccuracies of the anti-reflection coatings caused by the manufacturing process are investigated and their effect on transmission and reflection is studied. It is shown that these inaccuracies significantly deteriorate the electromagnetic properties of the window. In order to improve the characteristics, several investigations regarding geometrical deviations are performed and based on these analyses, an optimization of the window is carried out with simulations.**

I. Introduction

In radio astronomy interferometers, such as the Atacama Large Millimeter/sub-millimeter Array (ALMA), vacuum windows are used to establish a low-loss penetration of electromagnetic fields into cryostats which house the receiving units. Due to the reflection at the boundary between window and its surrounding, anti-reflection coatings (ARCs) are commonly applied on the dielectric to provide a low reflection and high transmission by matching the wave impedance of the window to that of free space. A broadband matching can be achieved when using gradient index (GRIN) coatings [1]. Thereby, the refraction index is gradually varied from the surrounding medium to the window medium using triangular grooves [2], for example. The numerical analysis of these structures can be accomplished by full-wave approaches like the finite element method (FEM) [3]. Although the periodicity of ARCs can be exploited by full-wave techniques, the computational effort is quiet high. A more efficient way is to use the rigorous coupled-wave technique [4]. For structures including a periodicity less than the wavelength, the effective medium theory (EMT) [5] can be applied, reducing the computation effort even more.

In this work, a prototype of vacuum windows for the ALMA Band 5 (163 –211 GHz) is analyzed using measurements, FEM, and an efficient semi-analytical approach based on EMT. The considered window consists of a solid disc made of high-density polyethylene (HDPE) and triangular wedge ARCs, with orthogonal orientation on both sides as illustrated in Fig. 1 (a)-(b). The window is manufactured by injection molding. Due to the non-optimized molding process and missing requirements for the tip geometry, the tips are not ideal triangular but possess a certain rounding as illustrated in Fig. 1 (c). The purpose of this contribution is to investigate the impact of such geometrical inaccuracies on the reflectivity and transmittance of injection molded windows. From these investigations, an optimized design for ALMA Band 5 vacuum windows is derived.

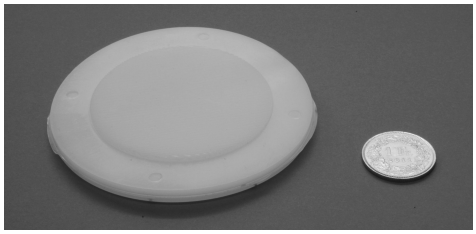

(a)

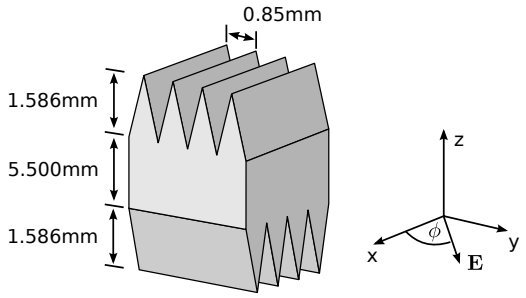

(b)

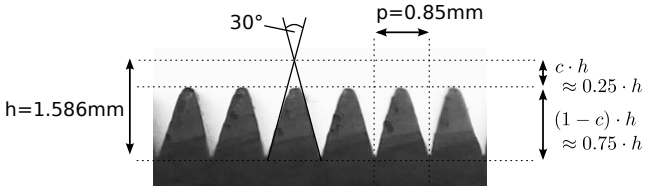

(c)

Fig. 1. Illustration of ALMA Band 5 vacuum window: (a) Photograph of the window. (b) Detailed view of the antireflection coatings which consist of ideal triangular grooves (design geometry) and illustration of the E-field polarization angle ϕ. (c) Microscopic picture of the real antireflection coating exhibiting rounded tips.

The remainder of this paper is organized as follows: section 2 briefly introduces the methods applied for investigations, section 3 shows numerical and experimental results concerning the reflectivity and transmittance of the prototype window. Section 4 analyzes several ARC geometries and proposes an optimized vacuum window. Finally, the main outcome of this work is concluded and a brief outlook on future activities is given.

II. Methods for Investigation

The techniques used for analyzing the vacuum window numerically and experimentally are sketched in the following.

A. Finite Element Method

A FEM-Solver [6] has been applied for numerical full-wave analysis. Here, the window was modelled by an infinite, periodic structure and it has been excited by Floquet modes.

B. Semi-Analytical Approach

As an alternative to full-wave solvers, we implemented an approach based on EMT. Following the derivations of [5], a one-dimensional periodic medium, consisting of dielectric slabs with ϵ_a and width a as well as dielectric slabs with ϵ_b and width b, can be approximated by an effective, isotropic medium. The associated zeroth-order approximations read

$$\epsilon_p^{(0)} = \frac{a\epsilon_a + b\epsilon_b}{a+b} \quad \text{and} \quad \epsilon_o^{(0)} = \frac{(a+b)\epsilon_a\epsilon_b}{a\epsilon_b + b\epsilon_a}, \quad (1)$$

where $\epsilon_p^{(0)}$ is valid if the E-field is parallel to the slabs and $\epsilon_o^{(0)}$ is valid if the E-field is orthogonal to the slabs. Second-order approximations, as derived by [5], can improve the accuracy. These approximations are valid as long as the wavelength exceeds the periodicity. To make use of the effective medium when treating GRINs, the anti-reflection profile is approximated by a staircase geometry, consisting of N segments, as illustrated in Fig. 2. From the segment dimensions, an effective

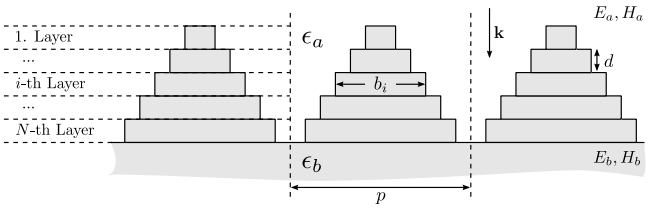

Fig. 2. Segmentation of a triangular ARC with pitch p at the interface between medium ϵ_a and medium ϵ_b. Each layer has a height d and the segment i has a width of b_i. Normal wave incidence $\mathbf{k}$ is considered.

material can be determined for each layer. With that, the initial problem is transferred into a multilayer problem with N homogeneous and isotropic layers. The effective permittivity of layer i is computed according to (1) with $a_i = p - b_i$. For solving this problem and normal wave incidence, we use a transfer matrix method which relates the fields on both sides of the ARC by

$$\begin{bmatrix} E_a \\ H_a \end{bmatrix} = \prod_{i=1}^{N} \begin{bmatrix} \cosh(jk_id) & Z_i \sinh(jk_id) \\ \frac{1}{Z_i}\sinh(jk_id) & \cosh(jk_id) \end{bmatrix} \cdot \begin{bmatrix} E_b \\ H_b \end{bmatrix}, \quad (2)$$

with Z_i being the characteristic impedance and k_i the complex wavenumber of the i-th layer. Here, the transmission matrices of each layer are multiplied to a single matrix. The reflection and transmission coefficients can be calculated from this expression.

C. Measurements

Measurements have been carried out in the frequency range between 140 GHz and 220 GHz using an ABmm vector network analyzer. For co-polar reflection measurements, the setup depicted in Fig. 3 was used. It consists of a transmitting corrugated feed horn, a first reflector, a $0°$ wire grid polarizer, a $45°$ wire grid polarizer, a second reflector, and a receiving corrugated horn. The same setup has been used for the cross-polar case with the exception that the $45°$ wire grid polarizer has been removed. The reflection measurements were calibrated with a short (flat aluminum reflector at the location of the device under test). Accurate transmission measurements could not be performed due to standing wave problems in the optical measurement setup. The beam waste is in the order of 10 mm which is a good representation of the beam size in the ALMA Band 5 optics.

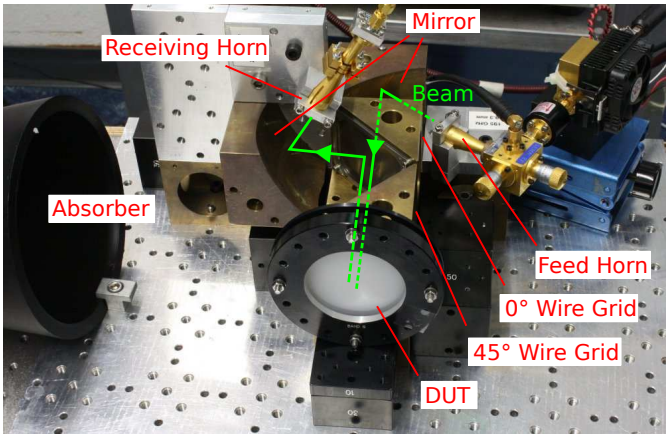

Fig. 3. Measurement setup used for the co-polar reflection measurements of the prototypes for ALMA Band 5 vacuum windows.

III. Analysis of the Prototype Vacuum Window

Before analyzing the prototype windows, we derived the permittivity by considering a solid HDPE disc without ARCs. From transmission measurements, we obtained a permittivity of $\epsilon = 2.323$ and a loss tangent of $\tan\delta = 2.3 \cdot 10^{-4}$ which agree well with data shown in [7]. In the numerical models, a homogeneous and isotropic material has been assumed. Each ARC was discretized by 101 elements in the semi-analytical approach and a second-order effective medium was used. The geometry has been meshed with curvelinear, second-order basis functions for FEM and a convergence criterion of 10^{-4} was applied. All investigations aimed at the frequency range 140 – 220 GHz and normal wave incidence. Multiple samples of the window have been tested and the measured results where reproducible.

The roundings of the tips are modelled by a fourth-order polynomial which has been approximately determined using the microscopic picture shown in Fig. 1. For simplicity, the degree of rounding shall be indicated by the parameter c as depicted in Fig. 1. In the present case, $c \approx 0.25$ which

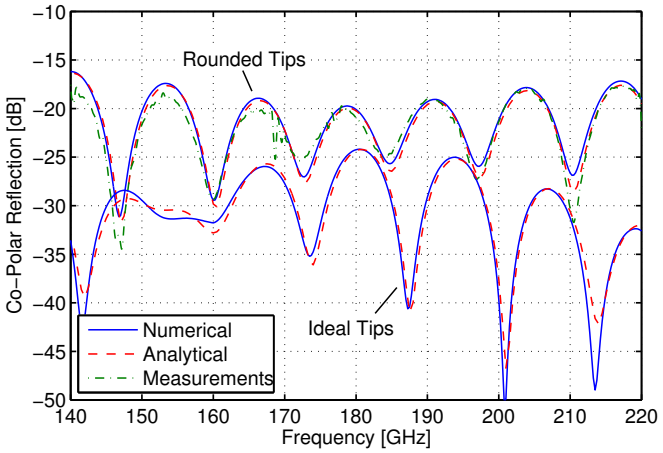

Fig. 4. Co-polar reflection for the vacuum window at normal incidence and a polarization of $\phi = 0°$. Results obtained by FEM (numerical), a semi-analytical approach (analytical) and measurements. Two different groove shapes are considered: rounded tips (real geometry) and ideal tips (design geometry), as illustrated in Fig. 1.

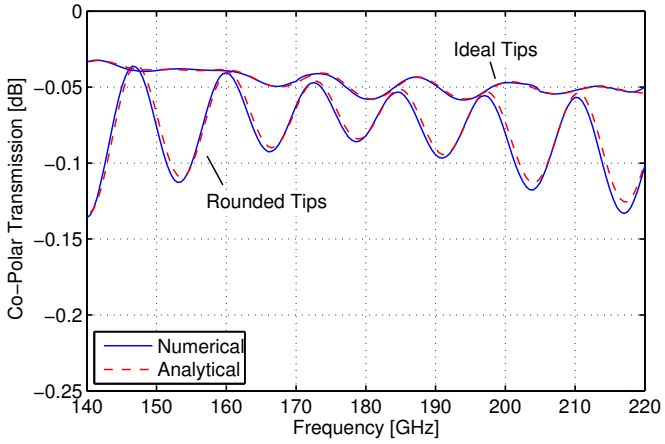

Fig. 5. Co-polar transmission for the vacuum window at normal incidence and a polarization of $\phi = 0°$. Results obtained by FEM (numerical) and a semi-analytical approach (analytical). Two different groove shapes are considered: rounded tips (real geometry) and ideal tips (design geometry), see Fig. 1.

means that the actual ARC height is only three-quarter of the prescribed height.

The first analysis puts its focus on an E-field polarization of $\phi = 0°$ where the field is parallel to the grooves on the illuminated side. Figure 4 shows the co-polar reflection obtained by simulations and measurements, respectively. The agreement between simulation results and measurements is very good. Also the semi-analytical approach agrees well with FEM. Moreover, Fig. 4 illustrates numerical results associated with ideal triangular grooves for comparison. One observes that the present rounding of tips degrades the reflection by, at least, 5 dB. Due to the imperfect tips, the ALMA Band 5 requirements for co-polar reflection, which prescribe -20 dB in the center 90% of the band, are not fulfilled by this prototype. Similar observations are made for the co-polar transmission shown in Fig. 5. Also here, the semi-analytical results agree very well with results obtained by FEM. In accordance with the co-polar reflection, the transmission is best for ideal triangular grooves. For this setup neither cross-polar reflection nor cross-polar transmission is predicted by the simulations. Contrarily, cross-polarization has been observed in the measurements. Moreover, birefringence of the HDPE is observed for the sample without ARCs which is also manufactured by injection molding. Here, the dominant orientation of birefringence coincides with the HDPE flow direction at the injection point.

The second analysis concerns a $\phi = 45°$ polarization of the E-Field with regard to the groove orientation. Figure 6 indicates that a good agreement between numerical and experimental results exists for co-polar reflection. In case of cross-polar reflection, a good agreement between FEM and measurements is observed, whereas the semi-analytical approach shows some deviations. In particular, a small error in the phase difference between the two orthogonal reflected modes, used for the $45°$ polarization, causes a deviation in

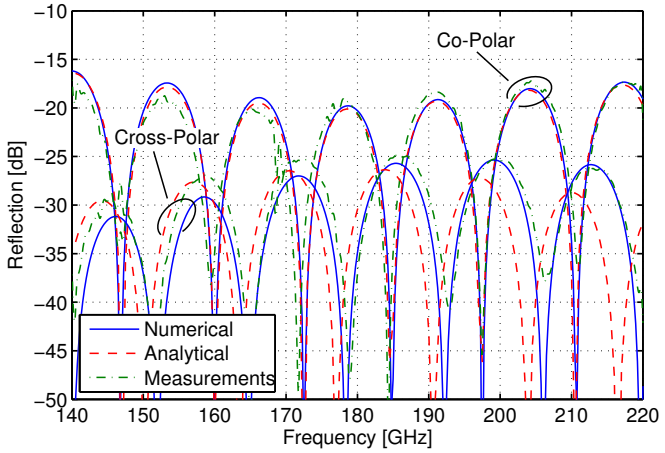

Fig. 6. Co- and cross polar reflection of the vacuum window with rounded tips at normal incidence and a polarization of $\phi = 45°$. Results obtained by FEM (numerical), a semi-analytical approach (analytical) and measurements.

the resonance frequencies. Nevertheless, the amplitude is well captured. Also in this case, no cross-polar transmission is predicted.

Computing 161 discrete frequency points took 3.3 h and 1 GB RAM for the FEM-Solver on 4 CPUs. The semi-analytical approach required 0.15 s on a single CPU and negligible amount of RAM.

IV. Optimization of the Vacuum Window

In order to improve the reflection properties of the considered vacuum window, some fundamental investigations have been carried out regarding the impact of geometrical variations on the reflectivity. For the following analysis, the same material as described above is used. In order to keep the ARC simple, triangular grooves are considered although other shapes such as quintic grooves [1] could be taken into account.

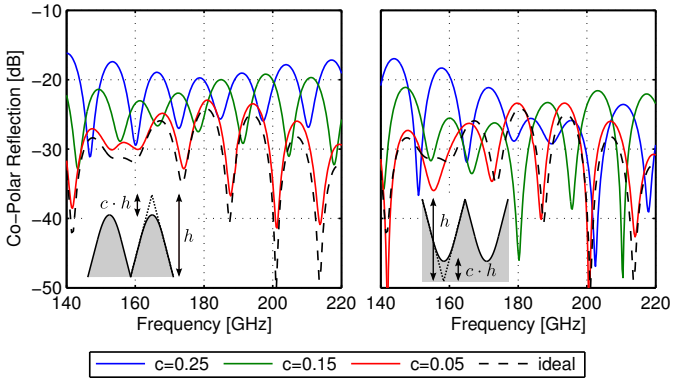

Fig. 7. Co-polar reflection of the vacuum windows with different grooves for normal incidence. *Left:* reflection depending on the rounding of the tips. *Right:* reflection depending on the rounding of the notch.

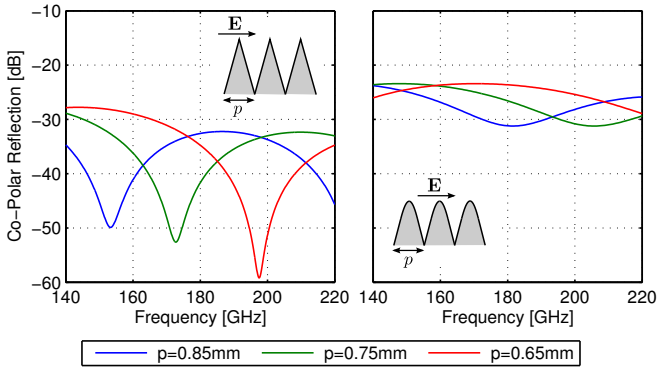

Fig. 8. Co-polar reflection of a single antireflection layer depending on the pitch p at normal incidence. *Left:* ideal triangular tip. *Right:* rounded tip with $c = 0.25$.

The first investigation concerns the influence of non-ideal tips and notches on the reflection of the vacuum window. Figure 7 shows the co-polar reflection coefficient for different roundings of the tip and notch, respectively. As depicted, the degree of rounding is described by the parameter c. Both cases indicate that deviations from an ideal triangular shape grow with an increasing rounding. In this example, roundings of the tip deteriorate the reflection more than roundings of the notch.

The second investigation regards the influence of the pitch on the minimum of the envelope of reflection. Only a single coated air-dielectric interface shall be considered in order to avoid resonances caused by the whole structure. The reflection associated with triangular grooves and rounded triangular grooves, respectively, is depicted in Figure 8. In both cases, the minimum is shifted towards higher frequencies with decreasing pitch and a fixed groove angle of 30°. This behavior is due to the decreasing profile depth which causes a reduction of the optical path length. Compared to rounded tips, the ideal grooves show a much more pronounced minimum.

By taking these investigations as a starting point, the initial prototype window has been optimized. The first step in this progress was to improve the manufacturing process such that tip rounding can be reduced to a value of $c = 0.1$, see Fig. 1

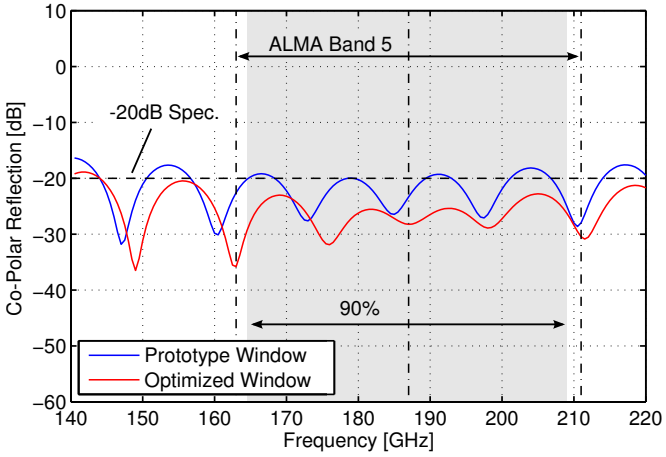

Fig. 9. Reflectivity of the prototype window and the optimized window for normal incidence. The grey coloured range refers to the center 90% of the ALMA Band 5 in which the reflection is required to be below -20 dB.

for the definition. With that, the overall co-polar reflection is reduced to less than -20 dB. In the second step, the minimum of the reflection envelope is shifted towards the ALMA Band 5 center (187 GHz) by changing the pitch from 0.85 mm to 0.7 mm. Figure 9 illustrates the co-polar reflection for the prototype window and the optimized window. The optimized window meets the required -20 dB in the center 90% of the band. Although not shown here, also the requirements for the transmission are fully met.

V. Conclusion

This paper investigates reflectivity and transmittance of prototypes for ALMA Band 5 vacuum windows by using numerical and experimental tests. Rounded tips of the considered ARC, which could be caused by the manufacturing process, deteriorate the electromagnetic properties of the window prototype. Several studies regarding different roundings are shown and a redesigned window with optimized reflectivity and transmittance is proposed.

The optimized window will be manufactured soon and measurements are planned to verify the numerically predicted reflection and transmission properties.

References

[1] W. H. Southwell, "Gradient-index antireflection coatings," *Optics letters*, vol. 8, no. 11, pp. 584–6, Nov. 1983.

[2] D. H. Raguin and G. M. Morris, "Analysis of antireflection-structured surfaces with continuous one-dimensional surface profiles." *Applied optics*, vol. 32, no. 14, pp. 2582–98, May 1993.

[3] J. Volakis, A. Chatterjee, and L. Kempel, *Finite Element Method Electromagnetics: Antennas, Microwave Circuits, and Scattering Applications*. New York, USA: Wiley, 1998.

[4] M. G. Moharam and T. K. Gaylord, "Rigorous coupled-wave analysis of planar-grating diffraction," *Journal of the Optical Society of America*, vol. 71, no. 7, p. 811, Jul. 1981.

[5] S. Rytov, "Electromagnetic properties of a finely stratified medium," *Soviet Physics JETP*, vol. 2, no. 3, pp. 466–475, 1956.

[6] Ansys, Inc. HFSS, Version 2015. [Online]. Available: http://www.ansys.com

[7] J. W. Lamb, "Miscellaneous data on materials for millimetre and submillimetre optics," *International Journal of Infrared and Millimeter Waves*, vol. 17, no. 12, pp. 1997–2034, 1996.